Available online at www.garmian.edu.krd

Passer Journal

Passer 5 (Issue 2) (2023) 218-223

http://passer.garmian.edu.krd/

Density Functional Theory Study of The Interaction Between a Nitrogen-Boron-Doped Graphene Nanosheet

Hemn Gharib Hussein[1*], Rangeen Othman Salih[1]

[1]*Department of Physics, College of Education, University of Sulaimani, Sulaimani, Kurdistan Region, Iraq.*

Received 06 February 2023; revised 28 April 2023;
accepted 29 Apil 2023; available online 30 April 2023

DOI: 10.24271/PSR.2023.384804.1249

ABSTRACT

The attractive interactions between Boron, B, and Nitrogen, N, codoped atoms in graphene nanosheets are calculated based on Density Functional Theory, DFT, using Quantum Espresso software, QE. We realized that the electron density distribution is strongly localized along B-N bonds when there is a strong attractive force between the dopant's atoms; however, when there is a lesser attractive force, the electrons are delocalized over the B-N bond of the hexagonal graphene ring. The molecular dynamic simulation is done to determine the thermal stability of the nanosheets. Additionally, since graphene is made up of a hexagonal structure, the locations of B or N atoms in para-, meta-, and ortho-positions are more sensitive. Furthermore, the symmetry of spin up and spin down of the band structure show that these monolayers are nonmagnetic materials. Moreover, we employed Phonopy software to demonstrate the specific heat capacity of the monolayers from 0 K to 1000 K, which is in the high-temperature limit. Based on our estimations, the BN-codoped graphene monolayers are beneficial in thermoelectric and optoelectronic devices.

Keywords: Density Functional Theory (DFT), Thermal Properties, Electronic Properties, Magnetic Properties, Graphene, Phonopy.

1. Introduction

The unique properties, zero-band gap and distinguishing physical characteristics, of graphene consisting of a plane sheet of carbon atoms with sp^2 hybridization led to improving the role of 2D device technology in the fields of thermo- and opto- electronics[1]. In fact, due to the special character of the band structure of graphene, its application in electronic devices is restricted. Several theoretical and experimental researches have been conducted to alter its electrical and, consequently, thermal properties. Numerous studies on graphene have been constructed to make heterostructures by adding Boron and Nitrogen atoms to it in place of its Carbon atoms[2-4], which can alter its band gap and thermal properties. Additionally, researchers[5, 6] noticed that by substituting B and N for carbon atoms, the physical features of the system's structure changed. It can be inferred that graphene has an extremely high heat conductivity[7]. A few years ago, several experimental[7–9] publications on heat transfer in graphene revealed extremely high thermal conductivity, which is important for applications like improving composite material thermal conductance and thermal management in electronic devices. Researchers have been looking for bandgap behavior, which is essential for thermal devices, in semiconducting materials in graphene systems. It is possible to accomplish this by expanding a bandgap that could result in effective devices[10, 11].

In addition, many studies have been done to modify the characteristics of pure graphene. A sizable alteration in the physical characteristics of graphene results from using of B and N dopant atoms. This is because of their close radii to carbon atoms, along with the resultant BN graphene semiconductor. Showing that the bonding between the B and N dopants in the BN graphene's physical properties is an attempt to demonstrate the impact of the dopant mixture on the material[12]. It has also been suggested that for weak attractive interactions, although the electrons in BN-codoped graphene are delocalized along the inter-hexagonal region, the strong attractive interactions cause the electron charge distribution to become extremely localized along B-N bonds[13]. In addition, the electronic structure of both doped systems around the Fermi energy has an impact on how well they respond optically, and the low energy range of the absorption spectrum is affected[14, 15]. When it comes to monolayer graphene that has been doped with B and N, from the infrared to the ultraviolet wavelength, the optical response advances and displays noticeable anisotropy for different polarizations[16, 17]. Also, it has been studied in[18] which pn-type semiconductors are beneficial for some devices such as thermoelectric, phonics and solar cell.

* Corresponding author
E-mail address: hemn.hussein@univsul.edu.iq (Instructor).
Peer-reviewed under the responsibility of the University of Garmian.

In this paper, we report the results of investigations carried out to further our understanding of how B-N delocalization affects electric, thermal and magnetic properties, we have focused on employing quantum espresso and Phonopy based on DFT formalism, which has a track record of being relied upon when modelling physical qualities. We have determined the thermal stability of pure and graphene with B-N doping. Due to the fact that phonons, which are either quanta or types of quasiparticles of the lattice vibrational energy, regulate their thermodynamic properties, it is crucial to thoroughly explore these features. It is crucial to evaluate these materials' heat capacities and simulate their molecular dynamics to solve this problem. We make an effort to determine the specific heat capacity and associated thermodynamic parameters of doped materials as a first step in this direction. The next section will give an explanation of the model and computational methodology. In section three, the analysis of the data results from the simulations was employed. In the last two sections, we report on the results of simulations on magnetic, optical and thermal properties.

2. Model and Computational tools

A 2 × 2 super-cell nanosheet consists of pure and BN-codoped graphene monolayer. First-principle calculations based on DFT within the Projector Augmented Wave, PAW, procedure implemented in the QE referring to the Quantum espresso, were performed[19, 20]. In addition, the generalized gradient approximation, GGA, is utilized to estimate the exchange and the correlation term with an assumption of Perdew-Burke-Ernzerhof-Solve, PBEsol[21]. The interaction between interlayers of graphene can be neglected by considering a vacuum length of 20 Å across the z-direction. The plane wave basis set is chosen to have a cut-off energy of 1000 eV, and the system is converged with the total energy in SCF (self-consistent field) cycles set at 106 eV and the forces on single atoms set at 0.001 eV/A. To determine the band structure and the DOS, respectively, we use the SCF and non-self-consistent field (NSCF) estimations. We also employed a Monkhorst-Pack grid with dimensions of 18 × 18 × 1 for the SCF and 100 × 100 × 1 for the NSCF[22]. Moreover, the Phonopy software conducts thermal simulations using DFT formalism. To avoid interlayer interactions, 32-atom simulated sheets of graphene are separated by a distance greater than 9.8 Å in the perpendicular direction. It is expected that the cut-off energy for plane waves is 816.34 eV. For sampling the BZ indicating the Brillouin zone, the Monkhorst-Pack technique is employed[23]. The structure is fully relaxed with a 4 × 4 × 1 k-point.

3. Results

3.1 Model and Band structure

Depending on the distance between the B and N atoms, this work employs three alternative district structures of BN-codoped graphene. Each type of BN-codoped graphene's atomic arrangement is shown in Fig. 1. The para-, ortho-, and meta-positions of a hexagonal ring are illustrated schematically in Fig. 1(a), and they were represented in[24, 25]. The N atom is in a meta-position in the initial configuration of our systems, known as BN-G-1, while the B atom is doped in an ortho-position. Fig. 1(b) displays how this configuration's atomic structures are distributed. The other two configurations, BN-G-2 Fig. 1(c) and BN-G-3 Fig.1 (d) have the N atom in a para- or a meta-position, respectively, with the B atom remaining in its ortho-position. In this manner, three BN graphene structures are formed, each with a distinct distance and level of contact linking the B and N atoms. In BN-G-1, BN-G-2, and BN-G-3, the distances connecting the B and the N atoms are 1.41, 2.43, and 2.8 A, respectively. Using SCF calculation to produce the total energy have used to establish the exchanging energy allying the B and N atoms[26, 27].

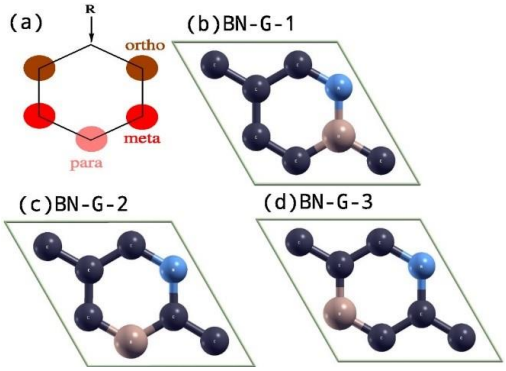

Figure 1: Diagram of hexagonal composition (a), and atomic configuration of 2×2×1 structure of BN-G-1(b), BN-G-2 (c), and BN-G-3 (d)

According to the findings, the far more energetically stable structure is the BN-G-1 structure. The amount of energy from SCF analyses are performed to assess the stability of the constructions. Our DFT analysis shows that the BN-G-1 structure's formation energy is (-191.721 eV), which is relatively lower than the values for the BN-G-2 structure (-190.533 eV) and the BN-G-3 structure (-190.644 eV). This demonstrates that the BN-G-1 structure is more stable energetically than the BN-G-2 and BN-G-3 structures. By using phonon computations, it is shown that the dynamics of our models are stable[28]. The dynamic matrix's eigenvalues are all positive, which suggests that the phonon band structure is dynamically stable. In addition, the band structure of BN-codoped graphene show that the band gap is opened due to interatomic interactions. Detailed information on the open band gap is presented in[28]. The zero band gap of pure graphene is changed to a specific value depending on the position of B and N dopant atoms in the structure. For instant, the band gap value of BN-G-1, BN-G-2, and BN-G-3 are 1.209, 0.133, and 1.273 eV, respectively. The values of band gap is very well agree with the literature[28] as Shown in Fig. 2.

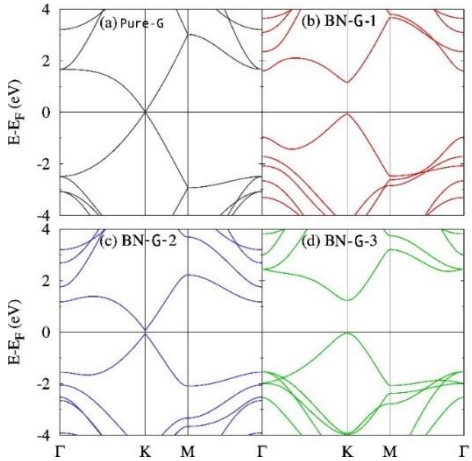

Figure 2: Pure-G (a), BN-codoped graphene (b), BN-G-2 (c), and BN-G-3 (d) configurations all have different electronic band structures[28].

3.2 Partial density of state (PDOS)

In Fig. 3, the partial densities of states (PDOS) for the BN-G-1, BN-G-2, and BN-G-3 structures are shown. The PDOS of the B and N atoms demonstrate that both dopant atoms contribute to the energy band gap opening, with the Fermi energy and the peaks and lowest of the valence and conduction band gaps in the energy range of -2 to 2 eV making a significant contribution. It is obvious that for pure graphene and BN-codoped materials, the four P_z π -bands surrounding the Fermi energy completely constitute the valence band maximum and the conduction band minimum. Furthermore, as would be predicted both to pure graphene and graphene doped with BN, the S and $P_{x,y}$ belong to the upper part of the conduction band and the bottom half of the valence band, respectively[29,30].

The BN-codoped graphene had a greater PDOS in all four cases, according to the analysis. The lower conduction bands are produced by the combined Pz of the C, B, and N atoms, whereas the valence bands are produced by the Pz of the C and B atoms. We see that the C atoms have a significant impact on the π-bands. More particular, the B and N atoms contribute somewhat more near the Fermi energy in the BN-G-1 and BN-G-3, which have a repelling interaction between them. Additionally, it is anticipated that the B and N atoms will contribute more to both the S and $P_{x,y}$ at the lower valence band. Additionally, it has been reported that raising the concentration of BN doping improves the coupling effect linking the C, B, and N atoms close to the Fermi level. These findings illustrate the possibility of using BN-codoped graphene systems in nanoelectronics by demonstrating how the doping interatomic interaction of BN graphene systems may substantially affect the electronic characteristics. Additionally, the altered band structures in the BN graphene formations modify the transition rates.

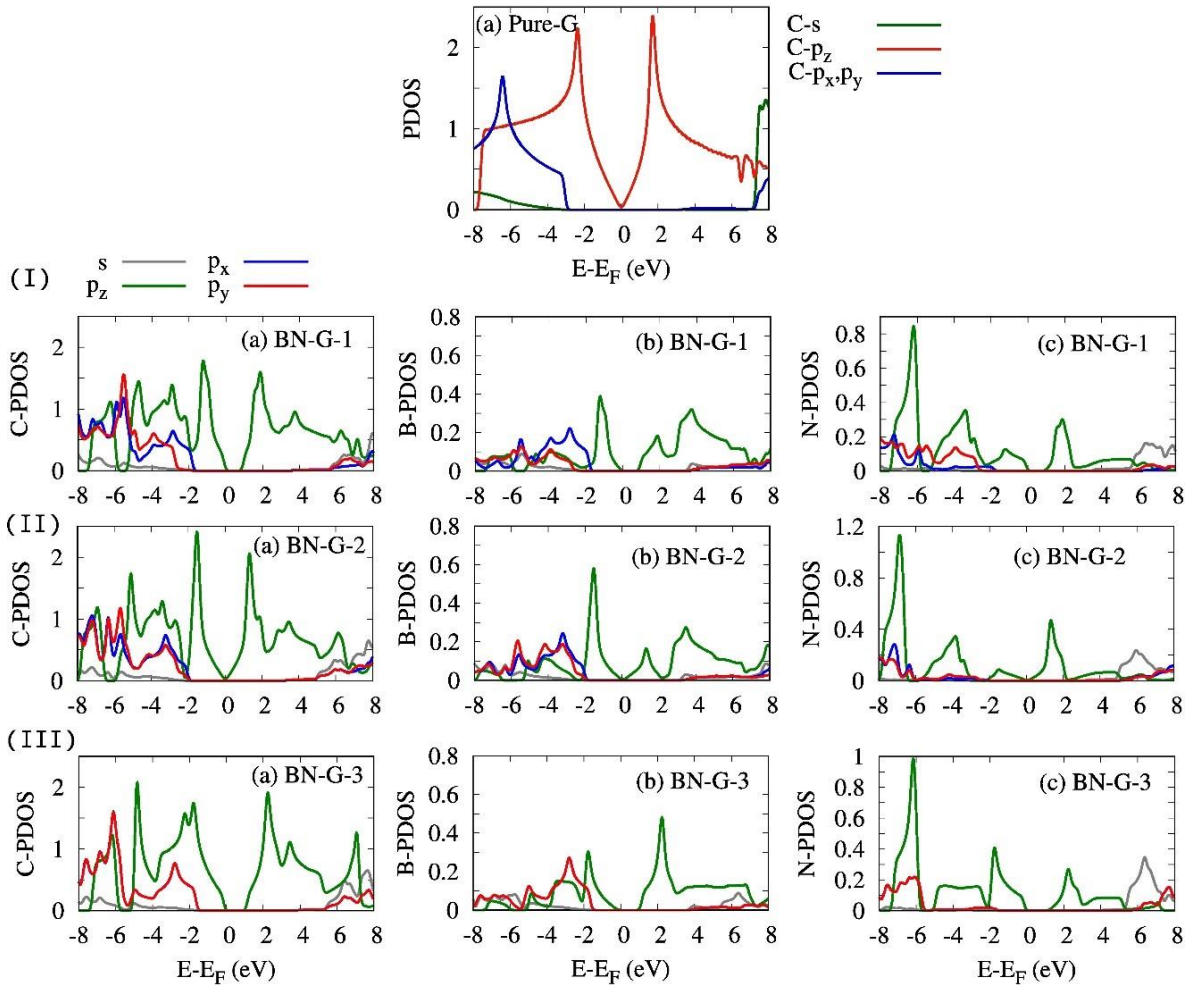

Figure 3: The partial densities of states (PDOS) for pure-G and BN-codoped (I, II, and III) are shown in (a-c).

3.3 Magnetic properties

Pure graphene was discovered to be non-magnetic since there was no magnetism present in the system. We calculated the magnetic properties of the BN codoped atom. The density of state or spin-dependent band structure calculations can be used to confirm the magnetic properties of the monolayers. Fig. 4, illustrates the BN-G-1, BNG-2, and BN G-3's spin-dependent densities of state for both spin up and spin down. Because band structures are symmetric, there is no spin splitting between spin up and spin down at the Fermi energy. The materials exhibit spin unpolarized semiconductor behavior, meaning that there is no spin separation seen between the spin up and spin down channels. As a result, these substances are referred to be nonmagnetic semiconductors.

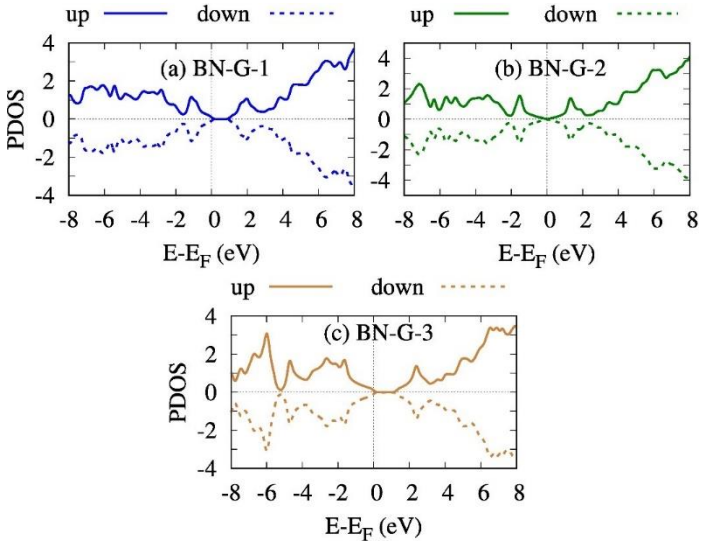

Figure 4: PDOS structure for the optimized BN-G-1, BN-G-2, and BN-G-3 structures, as well as for spin-up and spin-down (solid lines) (dashed lines). The Fermi energy is set to 0 and the energies are in terms of the Fermi level.

3.4 Thermal properties

In this section, the temperature-time curve as well as other thermal properties, specifically the heat capacity, are displayed including both pure and BN-codoped graphene monolayers. According to Fig. 5, the thermal stability is estimated with a time step of 1 fs up to 10 ps. At 300 K, neither the temperature curve for pure graphene monolayers nor that for BN graphene monolayers shows any significant temperature swings, structural disturbances, or bond breakage. This proves that the graphene monolayers are thermodynamically stable nanosheets, both in their natural state and when doped with BN. In addition, the total energy (orange line) of all four considered structures indicates energy conservation as the total energy fluctuation is less than 1.0 eV. We should mention that the second Y-axis (right-hand side axis) is the axis of the total energy, and it can be clearly seen that the fluctuation is less than 1.0 eV for all four structures.

The amount of heat absorbed by changes in temperature is referred to as a material's heat capacity. Fig. 6 displays the heat capacity of flat, pure, and BN-codoped graphene. At high temperatures, T > 700 K, the heat capacity remains nearly constant while temperature increases. Stronger bonds are anticipated to result in systems with higher heat capacities, in accordance with a tendency for the heat capacity predicted by classical theory[31]. This implies that a stronger binding structure can result in a higher heat capacity. An increase in the electronegativity differential across a bond actually makes it stronger.

The thermodynamic properties of doped and pristine graphene were then determined and compared. The specific heat capacity of pure graphene as computed by our calculations has been in comparison to actual data[32] and earlier calculations[33, 34] as shown in Fig. 6. It can be observed that the experimental data and the model match up well. According to the graph in Fig. 6, the specific heat for both pure and doped graphene approaches a constant value of 21 J/K/moll at temperatures as high as 1000 K[33, 34], which is equivalent to its Dulong-Petit value, but is only around 8 J/K/moll for pure graphene at normal temperatures of 300 K. When B and N are added to graphene at a 12.5% concentration, the specific heat values are similar to those of pure graphene, but there is only a minor difference in other parameters. It indicates that the dopant atoms slightly increase the heat capacity.

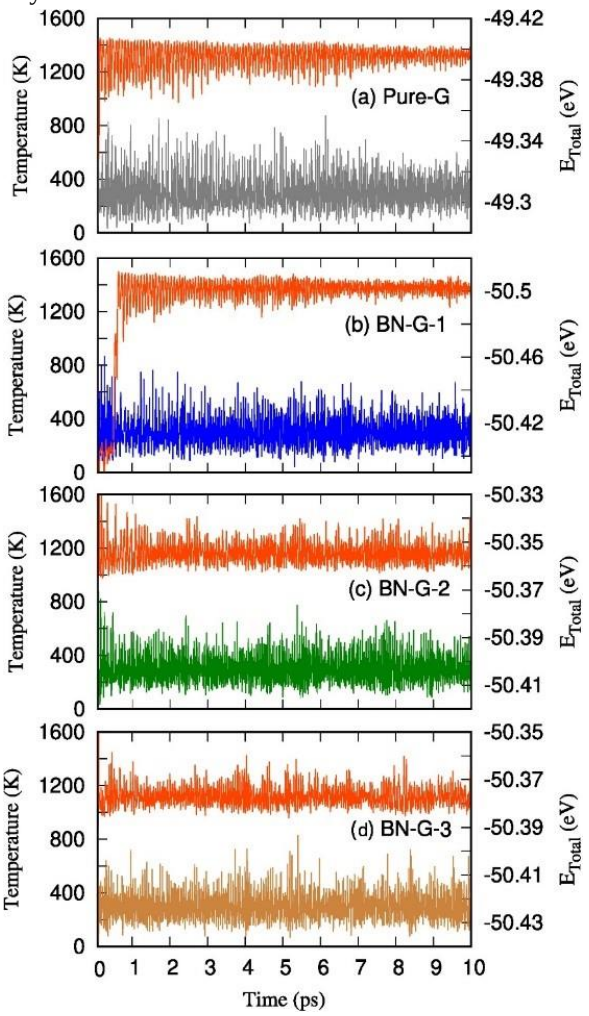

Figure 5: Temperature for optimal monolayers of pure and doped graphene against the AIMD simulation time steps at 300 K.

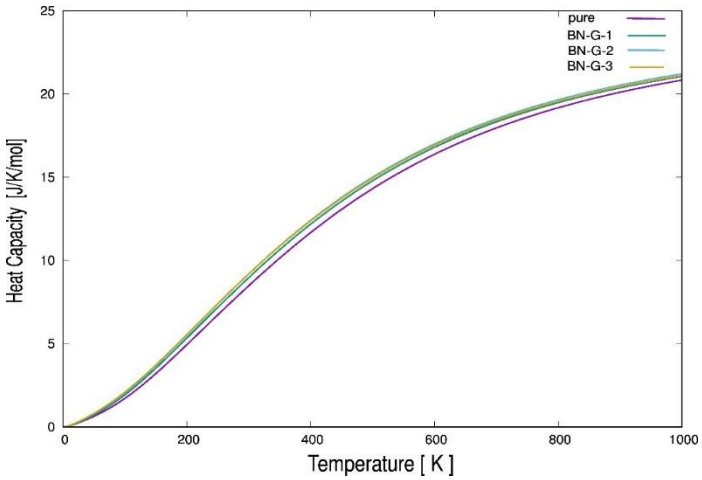

Figure 6: Heat capacity of the pure graphene and BN-codoped with temperature.

Conclusion

To conclude, Quantum Espresso and Phonopy software are used to study the molecular dynamics simulations to investigate the structural, thermal and magnetic characteristics of single layer graphene doped with boron and nitrogen atoms by monitoring the thermal stability of pure and dopant atoms at higher temperatures from 0 to 1000 K. Also, the impact of the attractive force between dopant atoms were highlighted. Depending on the attraction between dopant elements, several atomic combinations arise from different graphene structures have presumed. Additionally, these structures exhibit nonmagnetic semiconductor behavior due to their spin unpolarization and the absence of spin splitting between both spin up and spin down levels in their band configuration. By determining the specific heat based on thermal stability, we have been able to quantify BN graphene's unique performance with a broad bandgap. Therefore, this has been long recognized as important in thermoelectric devices. Finally, we have observed that the interaction between both B and N atoms may be controlled to manage the thermal characteristics of BN graphene, which may be advantageous for thermoelectric devices.

Conflict of interests

None

Acknowledgements

The authors acknowledge fruitful discussions with Nzar R. Abdulla from University of Sulaimani/College of Science/ Physics department.

Author contribution

The authors contributed equally to this work; form the implementation and design of the research, to the analysis of the results and to the writing of the manuscript.

Funding

The authors received no financial support for the research, authorship, and publication of this article.

References

1. K. S. Novoselov, A. K. Geim, S. V. Morozov and D. Jiang, Science, 2004, 306, 666.
2. P. Rani and V. K. Jindal, RSC Adv., 2013, 3, 802.
3. P. Rani and V. K. Jindal, Appl. Nanosci., 2014, 4, 989.
4. P.Rani, G. S. Dubey and V. K. Jindal, Phys. E, 2014, 62, 28.
5. Z. Weng-Sieh, K. Cherrey, N.G. Chopra, X. Blase, Y. Miyamoto, A. Rubio, M.L. Cohen, S.G. Louie, A. Zettl, R. Gronsky, Synthesis of bxcynz nano tubules, Phys. Rev. B 51 (1995) 11229 11232, https://doi .org /10 .1103 /PhysRevB .51.11229.
6. A. Rubio, J.L. Corkill, M.L. Cohen, Theory of graphitic boron nitride nanotubes, Phys. Rev. B 49 (1994) 5081–5084, https://doi .org /10 .1103 /PhysRevB .49 .5081.
7. S. Ghosh, I. Calizo, D. Teweldebrhan, E. P. Pokatilov, D. L. Nika, A. A. Balandin, W. Bao, F. Miao and C. N. Lau, Appl. Phys. Lett., 2008, 92, 151911.
8. W. Cai, A. L. Moore, Y. Zhu, X. Li, S. Chen, L. Shi and R. S. Ruoff, Nano Lett., 2010, 10, 1645.
9. J. H. Seol, I. Jo, A. L. Moore, L. Lindsay, Z. H. Aitken, M. T. Pettes, X. Li, Z. Yao, R. Huang, D. Broido, N. Mingo, R. S. Ruoff and L. Shi, Science, 2010, 328, 213.
10. Anukul K. Thakur, Klaudia Kurtyka, Mandira Majumder, Xiaoqin Yang, Huy Q. Ta, Alicja Bachmatiuk, Lijun Liu, Barbara Trzebicka, and Mark H. Rummeli. Recent Advances in Boron- and Nitrogen-Doped Carbon-Based Materials and Their Various Applications. Adv. Mater. Interfaces 2022, 9, 2101964. DOI: 10.1002/admi.202101964. https://doi.org/10.1002/admi.202101964.
11. Shubhda Srivastava, Prabir Pal, Durgesh Kumar Sharma, Sudhir Kumar, T. D. Senguttuvan, and Bipin Kumar Gupta. Ultrasensitive Boron−Nitrogen-Codoped CVD Graphene-Derived NO2 Gas Sensor. https://doi.org/10.1021/acsmaterialsau.2c00003 ACS Mater. Au 2022, 2, 356−366
12. N.R. Abdullah, H.O.Rashid, C-S Tang, A.Manolescu, V.Gudmundsson. Modelling electronic, mechanical, optical and thermal properties of graphene-like BC6N materials: Role of prominent BN-bonds. Physics Letters A 384 (2020) 126807. https://doi.org/10.1016/j.physleta.2020.126807
13. N.R. Abdullah, B.J. Abdullah, C.-S.Tang, V. Gudmundsson. Properties of BC6N monolayer derived by first-principle computation: Influences of interactions between dopant atoms on thermoelectric and optical properties. Materials Science in Semiconductor Processing 135 (2021) 106073. https://doi.org/10.1016/j.mssp.2021.106073
14. M. Goudarzi, S. Parhizgar, J. Beheshtian, Electronic and optical properties of vacancy and b, n, o and f doped graphene: Dft study, Opto-Electron. Rev. 27 (2) (2019) 130–136, http://dx.doi.org/10.1016/j.opelre.2019.05.002, URL https://www.sciencedirect.com/science/article/pii/S1230340218301021.
15. N.R. Abdullah, H.O. Rashid, C.-S. Tang, A. Manolescu, V. Gudmundsson, Conversion of the stacking orientation of bilayer graphene due to\ breaking the interaction of bn-dopants, 2021, arXiv preprint arXiv:2101.00462.
16. H. Bu, H. Zheng, H. Zhang, H. Yuan, J. Zhao, Optical properties of a hexagonal c/bn framework with sp2 and sp3 hybridized bonds, Sci. Rep. 10 (1) (2020) 6808, http://dx.doi.org/10.1038/s41598-020-63693-2.
17. N.R. Abdullah, H.O. Rashid, C.-S. Tang, A. Manolescu, V. Gudmundsson, Role of interlayer spacing on electronic, thermal and optical properties of bn-codoped bilayer graphene: Influence of the interlayer and the induced dipole-dipole interactions, J. Phys. Chem. Solids 155 (2021) 110095, https: //dx.doi.org/10.1016/j.jpcs.2021.110095, URL https://www.sciencedirect.com/ science/article/pii/S002236972100161X.
18. N.R. Abdullah, H.O. Rashid, M.T. Kareem, C.-S. Tang, A. Manolescu, V. Gudmundsson, Effects of bonded and non-bonded b/n codoping of graphene on its stability, interaction energy, electronic structure, and power factor, Phys. Lett. A 384 (12) (2020) 126350, http://dx.doi.org/10.1016/j.physleta.2020.126350, URL http://www.sciencedirect.com/science/article/pii/S0375960120301602.
19. R. Gebauer, U. Gerstmann, C. Gougoussis, A. Kokalj, M. Lazzeri, L. Martin-Samos, N. Marzari, F. Mauri, R. Mazzarello, S. Paolini, A. Pasquarello, L. Paulatto, C. Sbraccia, S. Scandolo, G. Sclauzero, A. P. Seitsonen, A. Smogunov, P. Umari, R. M. Wentzcovitch, QUANTUM ESPRESSO: a modular and open-source software project for quantum simulations of materials, Journal of Physics: Condensed Matter 21 (39) (2009) 395502. doi:10.1088/0953 8984/21/39/395502. URL https://doi.org/10.1088%2F0953-8984%2F21%2F39% 2F395502
20. P. Giannozzi, O. Andreussi, T. Brumme, O. Bunau, M. B. Nardelli, M. Calandra, R. Car, C. Cavazzoni, D. Ceresoli, M. Cococcioni, et al., Advanced capabilities for materials modelling with quantum espresso, Journal of Physics: Condensed Matter 29 (46) (2017) 465901.
21. G. Kresse, J. Furthm¨uller, Efficient iterative schemes for ab initio total-energy calculations using a plane-wave basis set, Phys. Rev. B 54 (1996) 11169–11186. doi:10.1103/PhysRevB.54.11169. URL https://link.aps.org/doi/10.1103/PhysRevB.54.11169
22. A. Togo, I. Tanaka, First-principles phonon calculations in materials science, Scripta Materialia 108 (2015) 1–5. doi: https: //doi.org/10.1016/j.scriptamat.2015.07.021. URL https://www.sciencedirect.com/science/article/pii/ S1359646215003127
23. H. J. Monkhorst and J. D. Pack, Phys. Rev. B: Condens. Matter Mater. Phys., 1976, 13, 5188.

24. N.R. Abdullah, D.A. Abdalla, T.Y. Ahmed, S.W. Abdulqadr, H.O. Rashid, Effect of bn dimers on the stability, electronic, and thermal properties of monolayer graphene, Results Phys. 18 (2020) 103282, http://dx.doi.org/10.1016/j.rinp.2020.103282, URL http://www.sciencedirect.com/science/article/ pii/S2211379720317496.

25. N.R. Abdullah, H.O. Rashid, C.-S. Tang, A. Manolescu, V. Gudmundsson, Properties of bsi6n monolayers derived by first-principle computation, Physica E (2020) 114556, http://dx.doi.org/10.1016/j.physe.2020.114556, URL http:// www.sciencedirect.com/science/article/pii/S1386947720316246.

26. N. Al-Aqtash, K.M. Al-Tarawneh, T. Tawalbeh, I. Vasiliev, Ab initio study of the interactions between boron and nitrogen dopants in graphene, J. Appl. Phys. 112 (3) (2012) 034304, http://dx.doi.org/10.1063/1.4742063, arXiv: https: //doi.org/10.1063/1.4742063.

27. N.R. Abdullah, H.O. Rashid, A. Manolescu, V. Gudmundsson, Interlayer interaction controlling the properties of ab- and aa-stacked bilayer graphene-like bc14n and si2c14, Surf. Interfaces 21 (2020) 100740, http://dx.doi.org/10.1016/j.surfin.2020.100740, URL http://www.sciencedirect.com/science/article/pii/S246802302030732X.

28. N.R. Abdullah, H.O. Rashid, C.-S. Tang, A. Manolescu, V. Gudmundsson, Modeling electronic, mechanical, optical and thermal properties of graphene-like bc6n materials: Role of prominent bn-bonds, Phys. Lett. A 384 (32) (2020) 126807, http://dx.doi.org/10.1016/j.physleta.2020.126807, URL ttp://www.sciencedirect.com/science/article/pii/S0375960120306745.

29. B. Mohan, A. Kumar, P. Ahluwalia, A first principle study of interband transitions and electron energy loss in mono and bilayer graphene: Effect of external electric field, Physica E: Low-dimensional Systems and Nanostructures 44 (7) (2012) 1670 – 1674. doi: https://doi.org/10.1016/j.physe.2012.04.017. URL http://www.sciencedirect.com/science/article/pii/ S1386947712001634

30. N. R. Abdullah, C.-S. Tang, A. Manolescu, V. Gudmundsson, Thermoelectric inversion in a resonant quantum dot-cavity system in the steady-state regime, Nanomaterials 9 (5) (2019) 741.

31. B. Mortazavi, F. Shojaei, T. Rabczuk, X. Zhuang, High tensile strength and thermal conductivity in BeO monolayer: A first-principles study, FlatChem

32. N. Mounet and N. Marzari, Phys. Rev. B: Condens. Matter Mater. Phys., 2005, 71, 205214.

33. E. Pop, V. Varshney and A. K. Roy, MRS Bull., 2012, 37, 1271.

34. D. Gray, A. McCaughan and B. Mookerji, Physics for SolidState Application, 2009, 6, 730.